RSC Advances

ROYAL SOCIETY OF CHEMISTRY

www.rsc.org/advances

Cite this: DOI: 10.1039/c0xx00000x

www.rsc.org/xxxxxx

ARTICLE TYPE

Stabilizing reconstruction induced by O protrusions of the ZnO (0001) polar surface

Yu Li,[a,b,c,d] Bo-Long Huang,[a] Rui-Qin Zhang,*[a] Zijing Lin,*[b] Michel A. Van Hove*[e]

Received (in XXX, XXX) Xth XXXXXXXXX 20XX, Accepted Xth XXXXXXXXX 20XX

DOI: 10.1039/b000000x

The stability of the ZnO polar surfaces which is crucial for their applications is still being debated intensely. Here, we demonstrate that O extrusion outside the outermost bilayer is a universal reconstruction behavior of the Zn-terminated (0001) surface (with or without terraces) to compensate the well-known instability of such polar surfaces. The study is based on first-principles energetics of several atomic reconstruction configurations that emerge spontaneously in ab-initio Molecular Dynamics simulations, including on-site O extrusions, O interstitials and O extrusions as adatoms at hollow sites, compared with previously proposed O-rich compensation models with O adatoms and Zn vacancies. The O extrusion process is specifically favored for Zn-rich environments, which provides a theoretical support of investigating the defect-process of ZnO polar surface.

1. Introduction

Zinc oxide (ZnO) is a transparent semiconductor with a wide band gap of about 3.2-3.44 eV [1, 2]. It has a wide range of applications, such as chemical sensors [3], catalysts [4-7], optoelectronics [8], nanowire lasers [9], diodes [10] and solar cells [11]. Meanwhile, low-dimensional ZnO nanostructures also have a number of applications due to their promising electronic and electromechanical properties [12-14] and can be utilized as piezoelectric sensors and electronic devices [15]. To further understand and develop these applications, controllable synthesis and growth of ZnO is a prerequisite; this in turn requires understanding the stability and driving force towards stabilization of its polar surfaces.

ZnO is an ionic crystal with hexagonal wurtzite structure, whose space group is $P6_{3mc}$. Clean and unreconstructed (i.e. bulk-like) surfaces of polar ionic crystal materials possess an intrinsic instability, since their successive layers have opposite charges arranged in bilayers: these bilayers collectively create a net dipole moment perpendicular to the surface, resulting in an unsustainable electrostatic energy which is in direct proportion to the macroscopic sample thickness if the opposite surfaces are not suitably restructured from their bulk-like form [16, 17]. A metallization of the surface [18] has been used and expected by a rearrangement of charges between the O- and the Zn-terminated surfaces. However, theoretical studies [16, 19, 20] concluded a contraction of the first Zn-O double layer from this metallization, which can be ruled out from experimental observation [30].To stabilize such polar surfaces, relevant theoretical studies have shown that, apart from situations where the adsorption of charged particles (e.g. H-passivation) occurs [19,21-22], stabilization is predominantly driven by surface reconstructions [4, 23-27]. For example, an outward relaxation of the topmost Zn layer is found and a 0.75 occupancy of the topmost Zn layer could best fit surface x-ray diffraction experiments for the ZnO(0001) surface [31, 32]. Unfortunately, the experiments gave no indication on how the removal of Zn atoms occurs. Following this, a theoretical prediction proposed that a 25% charge modification on both the O-terminated surface and the Zn-terminated surface can quench the overall dipole, independent of the slab thickness [33].

Other structures are also consistent with this compensation mechanism, such as existence of O adatoms and terraces and steps [24, 35]. However, the most recent published models based on STM results and calculations [4, 23-29] do not enable us to understand the process of the dynamic surface reconstruction itself. In particular, it is difficult to identify experimentally whether the O adatoms come from environmental adsorption, from molecular dissociation or from the ZnO system itself. A recent model, consistent with the observations, proposes a high density of cavities of various sizes on the surface, with Zn and O atoms leaving lattice sites, while the Zn atoms migrate freely on the surface and many O atoms are trapped at surface hollow sites forming adatoms [36]. Nonetheless, other stabilization mechanisms remain possible and need to be studied, which is the purpose of this work: we explore both stoichiometric and non-stoichiometric models using ab-initio molecular dynamics (MD) to "automatically" generate new possible structures and use these structures to reflect the stabilization mechanism from the aspects of dipole compensation and formation energies

Furthermore, to our knowledge, no ab-initio dynamic investigation of a clean and ideal ZnO(0001) polar surface has been undertaken. The ab-initio study from an ideally truncated surface may shed light on the essential dynamic mechanisms of reconstruction which are out of reach through current experimental approach. By contrast, multiple experimental processes can introduce dramatic defects and disorder on the otherwise regular surface, making the actual surface confusing to study in terms of its intrinsic driving force of stabilization. The fundamental structures observed in the ab-initio MD simulations may be considered to be typical and frequent in real complex

experimental conditions, despite the intrinsic simulation limitations compared to real experimental conditions, such as time scale and system size. The O-extrusion reconstruction which we predict in this work coincides with certain features of the adatom-cavity (ADC) structure recently proposed by Xu et al [36], which is based on a combination of low-temperature Scanning Tunnelling Microscopy (STM) and Low-Energy Electron Diffraction (LEED) experiments with static Density Functional Theory (DFT) calculations. Hence, our study can be the key to understanding and predicting the fundamental compensation mechanisms.

2. Computational Details

To illustrate the potential reconstruction and its influence on the surface stabilization, we carried out ab-initio MD simulations in this work. We used the Troullier-Martins pseudopotential [37] with the generalized gradient approximation (GGA) (Perdew-Burke-Ernzerhof functional [38, 39]) for DFT as implemented in the SIESTA package [40, 41]. A linear combination of numerical localized atomic orbitals (split-valence double-ζ basis set with polarization orbitals) was used as the basis representation of the Kohn and Sham wavefunctions [42]. In the MD calculations, an energy mesh cutoff of 200 Ry was used to calculate the charge density on a real-space grid mesh and only the Gamma point in k-space was calculated. The convergence criterion for the forces was set to be 0.02 eV/Å.

All surfaces were modelled by periodically repeated slabs with a thickness of four bilayers, separated by a vacuum layer of more than 15 Å, using a (4x4) two-dimensional unit cell. A dipole correction within the SIESTA code was used to prevent artificial electrostatic interactions between the repeated units and to compensate the electric field at the vacuum created by the dipole moment of the system. In our calculations, the dipole correction showed no noticeable influence on the structures generated by the MD simulations, but was necessary for static energy determination.

In order to study the stabilization behavior of the Zn-terminated surface, we build slab models for which the O-terminated back surface is stabilized according to electrostatic arguments [33]. A 0.5 monolayer (ML) of H is added as terminal hydroxyl (OH) groups on the unreconstructed O-terminated ZnO surface to stabilize this surface as previously proposed [43]. Calculations presented in this paper were performed by applying this compensation mechanism on the O surface. The MD simulations were performed under the conditions of a constant temperature and constant volume (NVT) ensemble using the Nosé–Hoover algorithm, with the two bilayers of the O-terminated surface (including the H atoms) held fixed with the bulk structure. A time step of 3 fs was used to integrate Newton's equation of motion and a smaller time step of 1 fs has also been tested and showed consistent results.

More importantly, there are two questions to which we have given special attention: (1) The reliability of the computational method, and (2) the Pulay force problem. Regarding the computational reliability: In the first-principles calculations, the SIESTA code uses localized basis sets to calculate the ZnO (0001) surface system (e.g. atomic coordinates, eigenvalues, atomic forces, etc.). Especially in the finite temperature MD simulations by first principles, the accuracy of the ion-ion and ion-electron interaction calculations will directly influence the MD results, as well as the accuracy of optimizations with total energy calculations. To prove the reliability of our work, we further used CASTEP [44], which is DFT software based on a pseudopotential method using plane wave basis sets, to implement the first-principles MD simulations with a high level of computation quality.

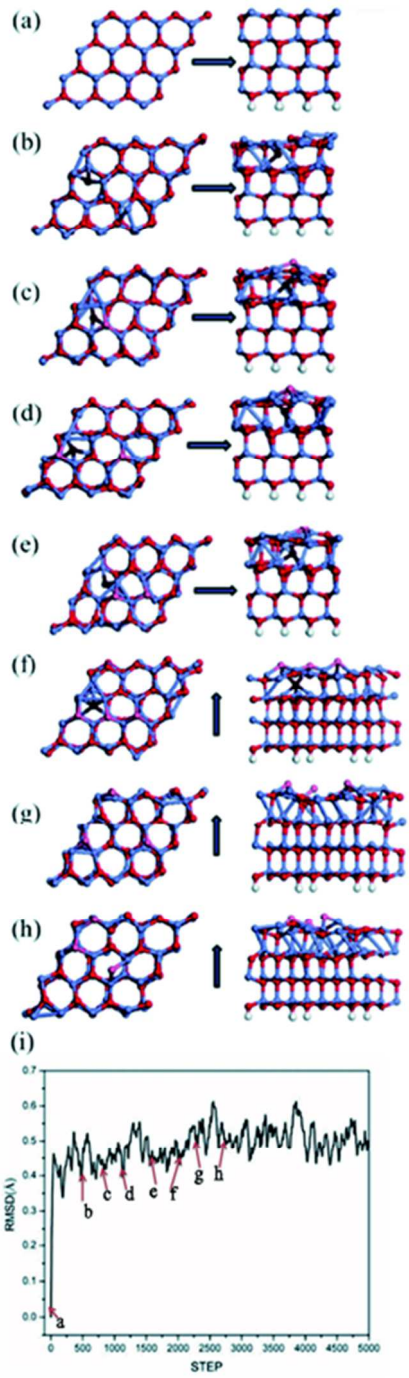

Fig. 1 Snapshots of typical reconstructed geometries in a MD run at 1600 K (O: red; Zn: gray; each left/right pairs show top and side views, resp., of a single (4x4) unit cell; as indicated by the arrows: (a) initial bulk-like structure at t = 0 ps, (b) O_{in} structure

(dark red) at t = 0.6 ps, (c) O_{ex}-O_{in} structure at t = 0.75 ps, (d) one O_{in} and two O_{ex} (light red) structures at t = 1.2 ps, (e) diffusion of O_{ex} at t = 1.65 ps, (f) one O_{in} and three O_{ex} structures at t = 1.95 ps, (g) three O_{ex} at t = 2.25 ps, and (h) three O_{ex}, among which one has diffused to a hollow site, at t = 2.7 ps. In (i) the RMSD of this trajectory is equilibrated after about 2000 steps (6ps).

We found that the results show great similarity between these two methods. In this complementary work, whether CASTEP uses density mixing or ensemble DFT (EDFT) [45] for electronic minimization and force optimization together with the BFGS algorithm for structural relaxation, the results objectively confirm the reliability of the work done with the SIESTA code. Regarding the Pulay force problem: Based on the Hellman-Feynman theorem, the force calculations in DFT are directly related to the ground state energy calculated using eigenstate wavefunctions expanded in a complete set of fixed basis functions. Meanwhile the basis set depends upon the ionic positions. The localized basis sets will contribute artificial so-called Pulay forces or stresses. Ideally, the Pulay forces will be minimized to zero in the limit of a complete basis set, but this is never realized in practice, or if position independent basis functions, such as plane-waves, are used. Therefore, the plane wave method can effectively solve this problem, as CASTEP does. However, regarding question (1) above, this shows that CASTEP also gives similar results, which confirms our findings. Therefore, the Pulay forces have a minor impact on our MD simulations, especially if we choose relatively large cut-off energy in the energy mesh for describing the charge density.

3. Results and Discussion

3.1. MD on pure Zn-terminated ZnO (0001)

As we will exhibit next, multiple types of surface reconstruction are observed in our MD simulations in a wide range of temperatures, including formation of adatoms, vacancies and interstitial defects. Coexistence and interaction among them are revealed. Interestingly, the Zn and O atoms show quite different dynamic behaviors, due to their different chemical bonding. A larger (6x6) unit cell with the same thickness also exhibits similar dynamic behaviors, while addition of a dipole moment correction in the calculation does not change the results, only increasing the accuracy of total energies.

Figure 1 shows MD snapshots of typical reconstructions of a Zn-terminated ZnO (0001) surface at nominally 1600 K within the first 3 ps of a single MD run. The bulk-like starting structure (Figure 1a) is a stack of identical bilayers (viewed sideways in the right-hand panel of Figure 1a), each consisting of one Zn layer and one deeper O layer. We observe intrusion of O atoms into interstitial sites (hereafter labeled "O_{in} structure", and colored dark red in Figure 1b-g) and onsite extrusion (without lateral displacement) of O atoms to positions outside the outermost bilayer (hereafter labeled "O_{ex} structure", and colored purple in Figure 1c-h). Thus, one oxygen atom (dark red in Figure 1b) has moved from the outermost bilayer into an interstitial site between the first and second bilayers as an interstitial defect ("O_{in} structure"). Soon after this intrusion of an O atom, the three Zn atoms adjacent to its initial site (now a vacancy) make new bonds with each other, forming a small Zn cluster (with Zn-Zn bond lengths between 2.4 and 2.6Å, relatively short compared to 2.67 Å for pure bulk Zn), as shown in Figure 1c. Concurrently, another nearby oxygen atom has moved outward as an extrusion, as shown in purple in Figure 1c (thus forming an "O_{in}-O_{ex} pair structure"). This outward movement may be due to local stress induced by the O_{in} and to O_{in}-O_{ex} repulsion.

After another 450 fs (see Figure 1d), the O_{ex} feature appears at another O site of the same hexagonal ZnO ring: this is not an atomic O shift (which would also need an O-O exchange), but a wave-like propagation of the extrusion between neighboring oxygen sites. At another random position (see Figure 1d), a second O atom has also been extruded directly at its own site ("O_{ex} structure"), without nearby O_{in}, concurrently with the formation of an in-plane Zn-Zn bond. Figures 1d-e also clearly show propagation of this O_{ex} feature, during which the first O_{ex} feature (see Figure 1e) propagates back to its initial O_{ex} site of Figure 1c. In Figure 1f, a second O_{ex} has formed near O_{in}, increasing the concentration of O_{ex} further from 12.5 % to 18.75 % (from two to three O_{ex} per (4x4) unit cell). This concentration of O_{ex} is equilibrated after 6ps as shown in the RMSD curve (Figure 1i). It is also noted that during the process described in Figures 1f~h, the sites of the three O_{ex} features propagate easily across the surface and one of the O atoms diffuses to a hollow site ("the O_{hollow} structure") while the O_{in} atom returns to a normal lattice position in the first bilayer. This process seems to play a role as an easy route for the appearance of O_{ex} structures.

Multiple MD simulations have been conducted at temperatures within the range 400-1300 K. They all reveal similar characteristics: random O_{ex} and O_{in} structures sometimes combined as O_{in}-O_{ex} pair structures, in a dynamic concentration from 1 to 4 such structures per (4x4) supercell. Such reconstruction occurs frequently already at relatively low temperatures, indicating a relatively small barrier. These reconstruction configurations have been confirmed to be local minima based on energy optimization, which will be discussed separately further below.

Besides the temperature, the initial model in MD simulations may also play an important role in determining the dynamic behavior. Apart from the bulk-like model containing equal numbers of Zn atoms and O atoms, the existence of Zn vacancies, O adatoms and steps are alternative reconstructions that might enhance the stability of the surface. Therefore, MD simulations starting from these specific models were performed using the same settings of computation parameters. Based on the compensation mechanism with 25% depletion of surface charges, the initial number of Zn vacancies and O adatoms was set between 1 and 4 (corresponding to a concentration of 25%) within a (4x4) supercell, corresponding to going from partial to complete compensation in principle [33]. These MD results confirm the existence of all the four typical local structures that we described above (O_{ex}, O_{in}, O_{hollow} and O_{ex}-O_{in} pair shown in Figure 1) and we accept them as universal reconstructions on the Zn-terminated polar surface of ZnO. Moreover, our MD results on the clean Zn-terminated ZnO (0001) surface show that the local structures of O_{ex} and O_{in} variations and propagations below

the topmost Zn-O bilayer drive the rearrangement and flattening of sub-surface Zn-O structures.

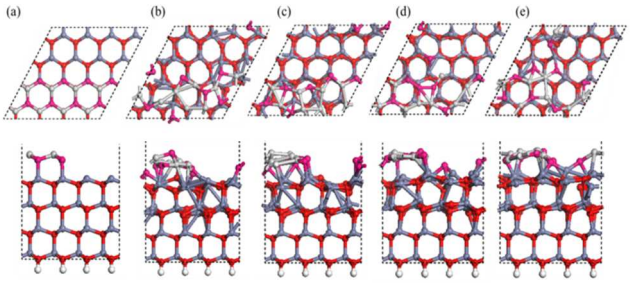

Fig.2 Snapshots of an MD simulation for the Zn-terminated surface with a bilayer-high step at 1600 K, in top and side views in top and bottom panels, respectively (the latter looking from the right side in the top view): (a) at 0 ps, (b) at 8.7 ps, (c) at 11.7 ps, (d) at 14.7 ps, (e) at 16.8 ps. (On the terraces, the Zn atoms are colored light grey and the O atoms purple to distinguish from others.)

3.2. MD on O-terminated nano-steps on ZnO (0001)

A previous Monte Carlo simulation has revealed possible surface reconstructions on the polar ZnO (0001) surface based on triangular islands and pits [27]. To understand the role of general nano-steps on the (0001) ZnO surface, we used a (4x4) supercell containing steps with a height corresponding to adding one Zn-O bilayer. Snapshots of our MD simulation at 1600 K are shown in Figure 2, starting again from a bulk-like surface. Figure 2b presents a rather chaotic situation, indicating intense mobility and reconstruction at the terrace after 0.9 ps (Figure 2b). An overall tendency appears whereby the O atoms at the terrace gradually move outward to form O-rich step edges, leaving Zn-rich regions within the upper terraces (see Figure 2c-e). The diffusion process is through onsite extrusion and diffusion of O (to hollow sites), from the outer step edges to the concave in-step regions. This reconstructed O terminated step edge is similar to previous results [27] for triangular terraces.

Based upon our MD simulations, we conclude that the O_{ex} reconstruction can be considered as a universal feature on this polar surface, even in the presence of available Zn vacancies, O adatoms, or nano-steps. Admittedly, the relative total energies of these reconstructed configurations cannot be obtained through MD simulations. Therefore, we optimized these specific models with DFT, using improved parameters compared to the MD simulation, consistent with previous reports [39]. An energy mesh cutoff of 300 Ry and a 6x6x1 k-sampling generated by the Monkhorst-Pack scheme for the first Brillouin zone were used after testing convergence.

3.3. Modification by reconstructions

We used a (2x2) slab model (corresponding to a 1/4 ratio of defects; we also tested a (4x4) unit cell to prove sufficiency of size) with a vacuum region of more than 15 Å to represent the reconstructed surfaces observed in the MD simulation (see Figure 3). Here the thickness of the slab was increased to eight Zn-O double layers[24]. All slabs were optimized at 0K with the back four double layers and H atoms fixed. A perfectly ordered, defect-free surface (as shown in Figure 3a) was also relaxed as a reference. We will discuss the compensation preferences of various reconstruction mechanisms by comparison between those structures in terms of stability and polarity.

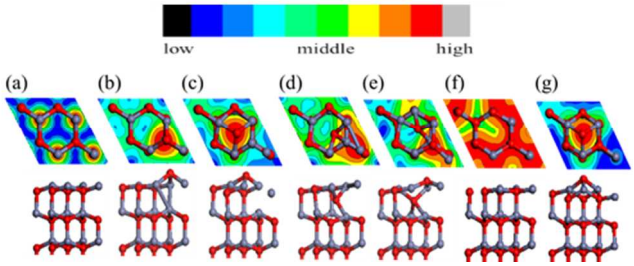

Fig.3 Top and side views of optimized structures at 0K for bulk-like and reconstructed models of Zn-terminated ZnO(0001), in top and side views in the top and bottom panels, respectively (showing only the outermost 3 of 8 bilayers and one (2x2) unit cell): a) the bulk-like surface; b) the O_{ex} structure; c) the O_{hollow} structure; d) the O_{in} structure; e) the O_{ex}-O_{in} pair structure; f) the Zn vacancy structure, g) the O adatom structure at the hollow site. All the relaxed structures are overlaid on top of simulated scanning tunneling microscopy (STM) images in constant current mode (showing the isosurface of constant charge density ρ = 0.002 e/Bohr^3, with heights colored according to the color bar).

Table 1. Relative energies and electric dipole moments of different models of the ZnO(0001) surface. The total energy of the optimized bulk-like ZnO model of Fig. 3a is set as reference (0 eV).

Structure	bulk-like	O_{ex}	O_{hollow}	O_{in}	O_{ex}-O_{in}
Relative energy(eV)	0	-0.18	0.08	0.44	0.65
Electric dipole moment (a.u.)	0.67	-0.04	-0.43	0.02	-0.23

The calculated interlayer distances for the bulk-like surface show similar tendencies as in previous reports [9, 10, 16, 39]: the interlayer spacing d_{12} (within the outermost ZnO bilayer) is clearly reduced by 26% from the bulk value, while the next spacing d_{23} (between the outermost two ZnO bilayers) shows a 4.2% expansion vs. the bulk. In fact, for all the reconstructed structures, the average spacing within the outermost bilayer is significantly reduced relative to the bulk, while the average spacing between the outermost two bilayers also increases. The energetic results and electric dipole moments (perpendicular to the surface) of these structures are listed in Table 1, with the energy of the optimized bulk-like structure of Fig. 3a as reference.

We find that the O_{ex} structure is more favorable than the bulk-like model by 0.18 eV and also has a negligible dipole moment. In contrast, the other reconstructions have unfavorable energies, though all exhibit a quenched dipole moment in the z direction. We even find overcompensation (negative dipole) for the O_{hollow} and O_{ex}-O_{in} structures. Though such overcompensation does not exist for the O_{in} structure, the strong stress induced by the O_{in}

atom increases the total energy. This suggests a competition between bonding character and polarity for the final stability of these structures, which shows agreement with recent calculations by Xu et al [36].

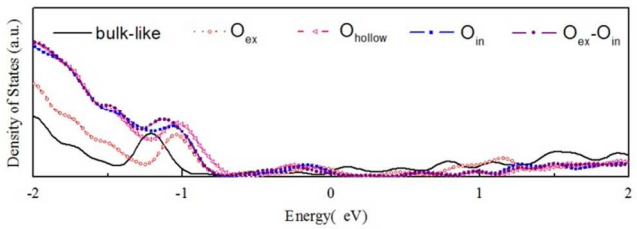

Fig.4 Total density of states (TDOS, in arbitrary unit) of (a) the optimized bulk-like ZnO surface, (b) the optimized O_{ex} model, (c) the optimized O_{hollow} model, (d) the optimized O_{in} model and (e) the optimized O_{in}-O_{ex} model.

Table 2. Total energies of various compensation systems, relative to the optimized bulk-like ZnO model of Fig. 3a. The O_2 gas and Zn gas correspond to the O-rich/Zn-poor limit; Zn bulk corresponds to the Zn-rich/O-poor limit, indicating a clustering of abundant Zn atoms.

Structure	*Total energy (Zn rich: Zn bulk)*	*Total energy (O rich: O_2 gas)*	*Total energy (O rich:: Zn gas)*
Bulk-like	0.18	0.18	0.18
O_{ex}	**0**	0	**0**
Zn_{vac}+Zn	0.35	----------	3
O_{adatom}-O	----------	**-3.76**	----------

In Figure 4 we display the density of states (DOS) calculated for the initial bulk-like model and the reconstructed models illustrated in Figure 1. The main change of the DOS curve occurs at the localized peak around -1 eV, which corresponds to the outermost O atoms. Another electronic modification is found around the Fermi energy, indicating the existence of dangling bond electronic states on the surface. Both of the two variations are expected and proved to come from the surface reconstructions based on a localized density of states (LDOS) analysis. All the models show metallic properties, due to the limited thickness of the slab. Besides, the different O-complex structures on the surface show variations of the DOS spectra near -1eV compared to the DOS spectra of the bulk-like structure, which represents modification of the electronic structure by local reconstructions.

We now focus on the O_{ex} structure since it is a potential stabilizing mechanism for this polar surface of ZnO. The extruded O breaks a bond with a deeper Zn atom while it maintains three O-Zn bonds closer to the surface plane. To saturate the valence electrons, the Zn atom beneath the extruded O makes new bonds with Zn atoms of the outermost layer. The outward displacement of the O atom is able to quench the overall dipole moment (in the +z direction), by inducing an opposing electric dipole in the –z direction. The concentration of O_{ex} as well as its effect on the overall dipole moment has been tested. A density of defects higher than the 25% shown in Figure 3b is energetically unstable, indicating a strong repulsion between neighboring O_{ex} atoms. Such an upper concentration limit also exists for the other structures. In contrast, any lower concentration of O_{ex} structures will not compensate the dipole moment completely, e.g. 12.5% of O_{ex} will leave a dipole moment of 0.27 a.u. per unit cell higher than 25% of O_{ex} (whose dipole is set as 0 in Table 2). As a result, the favorable concentration of 25% is in agreement with the former experimental [31, 32] and theoretical results [33] of charge transfer. Experimentally, the source of the observed O adatoms is unclear. Our findings suggest that the O_{ex} is a potential source of an O adatom, which escapes from ZnO surface layers and diffuses to the hollow site. In Figure 3, we present simulated STM images of all the candidate reconstructions for comparison with experimental observations. The STM simulations were determined with a constant current mode using the Tersoff-Hamann approximation.

A comparison of formation energies has also been conducted between this stabilization mechanism and two earlier compensation models: the isolated O-adatom and the Zn-vacancy models. To this end, the chemical potentials of O_2 gas, Zn gas and Zn bulk were involved, corresponding to various experimental conditions. The chemical potential of "O_2 gas" as a reference implies that oxygen is abundantly available in the gas phase, while "Zn gas" is used to represent the absence of Zn atoms from the surface. Both of these imply an O-rich limit, while "Zn bulk" indicates abundant Zn atoms clustering on the ZnO surface as the Zn-rich limit. Table 2 summarizes the total energies of various compensation models, for these experimental limits. The total energy of O_{ex} is set as the energy reference (0 eV) and a negative energy indicates a higher stability. As Table 2 indicates, the O_{ex} structure is favorable compared to the other stability mechanisms for the Zn-rich condition as well as the Zn-poor condition referenced to Zn gas. On the contrary, for the O-rich condition referenced to the O_2 gas, the O adatom model is much better than the others. This result also confirms the feasibility of O_{ex} as a stability mechanism.

Conclusions

In conclusion, we have studied the dynamic behavior of the Zn-terminated polar surface ZnO(0001) by ab-initio MD simulations, which reveal several atomic reconstructions at elevated temperatures. O atoms tend to be pushed out from the surface as extrusions. These extrusions may be the main source of O adatoms at the top sites or hollow sites, leaving vacancies at the initial O sites. Based on our MD simulations, reliable optimization and energy analysis support these O extrusions as a stabilizing reconstruction mechanism, especially in the Zn-rich limit. Our work reveals novel defects such as the O_{ex} and O_{in} structures and predicts their ability to compensate for the intrinsically destabilizing dipole moments of bulk-like surface structures.

Acknowledgements

The work described in this paper is supported in part by a grant from the Research Grants Council of Hong Kong SAR [Project No. CityU 103511], by the State Key Development Program for Basic Research of China (Grant No. 2012CB215405), by the National Natural Science Foundation of China (Grant No. 11074233), by the Natural Science Foundation of SZU (grant no. 836-000064), by the Hong Kong Baptist University Strategic Development Fund and by the High Performance Cluster

Computing Centre, Hong Kong Baptist University, which receives funding from the Research Grants Council, University Grants Committee of the HKSAR and Hong Kong Baptist University.

Notes and references

[a] *Department of Physics and Materials Science, City University of Hong Kong, Hong Kong SAR, China. E-mail: aprqz@cityu.edu.hk*
[b] *Department of Physics, University of Science and Technology of China, Hefei, China. E-mail: zjlin@ustc.edu.cn*
[c] *USTC-CityU Joint Advanced Research Centre, Suzhou, 215123, China*
[d] *College of Materials Science and Engineering, Shenzhen University, Shenzhen, China* [e] *Institute of Computational and Theoretical Studies & Department of Physics, Hong Kong Baptist University, Hong Kong SAR, China. E-mail: vanhove@hkbu.edu.hk*

1 F. Fuchs, J. Furthmüller, F. Bechstedt, M. Shishkin, and G. Kresse, *Phys. Rev. B,* 2007, **76**, 115109.
2 J. Wróbel, K. J. Kurzydłowski, K. Hummer, G. Kresse, and J. Piechota, *Phys. Rev. B,* 2009, **80**, 155124 .
3 W. Göpel, *Prog. Surf. Sci.* , 1985, **20** (1), 9.
4 O. Dulub, L. A. Boatner and U. Diebold, *Surf. Sci.* , 2002, **519** (3), 201.
5 T. S. Askgaard, J. K. Nørskov, C. V. Ovesen and P. Stoltze, *J. Catal.* ,1995, **156** (2), 229.
6 I. Nakamura, T. Fujitani, T. Uchijima and J. Nakamura, *J. Vac. Sci. Technol. A-Vac. Surf. Films,*1996 , **14** (3), 1464.
7 M. Bowker, H. Houghton and K. C. Waugh, *Journal of the Chemical Society-Faraday Transactions* I, 1981, **77**, 3023.
8 L. J. Brillson and Y. C. Lu, *J. Appl. Phys.* ,2011, **109** (12)121301.
9 D. Vanmaekelbergh and L. K. van Vugt, *Nanoscale,* 2011, **3** (7), 2783.
10 D. M. Bagnall, Y. F. Chen, Z. Zhu, T. Yao, S. Koyama, M. Y. Shen and T. Goto, *Appl. Phys. Lett.,* 1997, **70** (17), 2230.
11 J. S. Wu and D. F. Xue, Sci. Technol. *Adv. Mater.* , 2011, **3**, 127.
12 X. Wang, J. Song, J. Liu, and Z. L. Wang, *Science,* 2007, **316** (5821), 102.
13 J. Zhou, Y. Gu, P. Fei, W. Mai, Y. Gao, R. Yang, G. Bao, and Z. L. Wang, *Nano. Lett.* 2008, **8** (9), 3035.
14 J. H. He, C. L. Hsin, J. Liu, L. J. Chen, and Z. L. Wang, *Adv. Mater.* ,2007, **19** (6), 781.
15 H. Xue, N. Pan, M. Li, Y. Wu, X. Wang, and J. Hou, *Nanotechnology* **21** (21), 215701 (2010); X. Wang, J. Zhou, J. Song, J. Liu, N. Xu, and Z. L. Wang, *Nano. Lett.* **,**2006, **6**, 2768.
16 C. Noguera, *J. Phys.-Condens. Mat*., 2000, **12** (31), R367.
17 J. Goniakowski, F. Finocchi and C. Noguera, *Rep. Prog. Phys.*, 2008, **71** (1).
18 A. Wander, F. Schedin, P. Steadman, A. Norris, R. McGrath, T. S. Turner, G. Thornton, and N. M. Harrison, *Phys. Rev. Lett.,* 2001, **86**, 3811.
19 A. Wander and N. M. Harrison, *J. Chem. Phys.,* 2001, **115**, 2312.
20 M. Valtiner, M. Todorova, G. Grundmeier, and J. Neugebauer, *Phys. Rev. Lett.* **103**, 065502 (2009).
21 M. Valtiner, M. Todorova, and J. Neugebauer, *Phys. Rev. B,* 2010, **82**, 165418.
22 J. M. Carlsson, *Comp. Mater. Sci,* 2001, **22** (1-2), 24.
23 O. Dulub, U. Diebold, and G. Kresse, *Phys. Rev. Lett.,* 2003, **90**, 016102.
24 G. Kresse, O. Dulub, and U. Diebold, *Phys. Rev. B,* 2003, **68**, 245409.
25 F. Ostendorf, S. Torbrügge, and M. Reichling, *Phys. Rev. B,* 2008, **77**, 041405 (R).
26 S. Torbrügge, F. Ostendorf, and M. Reichling, *J. Phys. Chem. C* 2009, **113**, 4909.
27 J. V. Lauritsen, S. Porsgaard, M. K. Rasmussen, M. C. R. Jensen, R. Bechstein, K. Meinander, B. S. Clausen, S. Helveg, R. Wahl, G. Kresse, and F. Besenbacher, *ACS Nano,* 2011, **5**, 5987.
28 H. Meskine and P. A. Mulheran, *Phys. Rev. B,*2011, **84**, 165430.
29 S. Pal, T. Jasper-Tönnies, M. Hack, and E. Pehlke, *Phys. Rev. B,* 2013, **87**, 085445.
30 M. Sambi, G. Granozzi, G. A. Rizzi, M. Casarin and E. Tondello, *Surf. Sci.* 1994.**319** (1-2), 149.
31 H. Maki, N. Ichinose, N. Ohashi, H. Haneda and J. Tanaka, *Surf. Sci.,* 2000, **457** (3), 377.
32 N. Jedrecy, M. Sauvage-Simkin and R. Pinchaux, *Appl. Surf. Sci.*, 2000, **162**, 69.
33 B. Meyer and D. Marx, *Phys. Rev. B,* 2003, **67** (3), 035403.
34 S. Torbrugge, F. Ostendorf and M. Reichling, *J. Phys. Chem. C,* 2009, **113** (12), 4909.
35 H. Xu, L. Dong, X. Q. Shi, M. A. Van Hove, W. K. Ho, N. Lin, H. S. Wu, and S. Y. Tong, *Phys. Rev. B*, 2014, **89** 235403.
36 N. Troullier and J. L. Martins, *Phys. Rev. B,* 1991, **43** (3), 1993.
37 J. P. Perdew, K. Burke and M. Ernzerhof, *Phys. Rev. Lett.,* 1996, **77** (18), 3865.
38 J. P. Perdew, K. Burke and M. Ernzerhof, *Phys. Rev. Lett.*,1997, **78** (7), 1396.
39 P. Ordejon, E. Artacho and J. M. Soler, *Phys. Rev. B,* 1996, **53** (16), 10441.
40 J. M. Soler, E. Artacho, J. D. Gale, A. Garcia, J. Junquera, P. Ordejon and D. Sanchez-Portal, *J. Phys-Condens. Mat.,* 2002, **14** (11), 2745.
41 W. Kohn and L. J. Sham, *Phys. Rev.* ,1965, **140** (4A), A1133.
42 B. Meyer, *Phys. Rev. B* , 2004, **69** (4), 045416.
43 S. J. Clark, M. D. Segall, C. J. Pickard, P. J. Hasnip, M. J. Probert, K. Refson, and M. C. Payne, *Zeitschrift für Kristallographie,* 2005, **220**, 567.
44 N. Marzari, D. Vanderbilt, and M. C. Payne, *Phys. Rev. Lett.,* 1997, **79**, 1337.